Biodegradation of different bioplastics by specialised microbial communities in a coastal brackish environment

Igor S. Pessi[1,2,3,#,†], Eeva Eronen-Rasimus[1,2,#], Pinja Näkki[1], David N. Thomas[4,3], and Hermanni Kaartokallio[1]

[1]Marine and Freshwater Unit, Finnish Environment Institute (Syke), Helsinki, Finland
[2]Department of Microbiology, University of Helsinki, Helsinki, Finland
[3]Helsinki Institute of Sustainability Science (HELSUS), Helsinki, Finland
[4]Faculty of Biological and Environmental Sciences, University of Helsinki, Helsinki, Finland
[#]Both authors contributed equally to this work
[†]Corresponding author: igor.pessi@gmail.com

Igor S. Pessi: https://orcid.org/0000-0001-5926-7496
Eeva Eronen-Rasimus: https://orcid.org/0000-0002-1749-0793
Pinja Näkki: https://orcid.org/0000-0003-2499-4751
David N. Thomas: https://orcid.org/0000-0001-8832-5907
Hermanni Kaartokallio: https://orcid.org/0000-0002-3650-4628

Running title: Bioplastic biodegradation in the Baltic Sea

Abstract

Bioplastics are frequently promoted as a more sustainable alternative to conventional plastics. Microorganisms are metabolically versatile and central to marine ecosystems, yet the potential of marine microbial communities to degrade different bioplastics and the effect of environmental factors are poorly understood. Employing multi-seasonal *in situ* and *in vitro* experiments, we assessed the biodegradation of six bio-based bioplastic materials in the brackish Baltic Sea and characterised the associated microbial communities with metagenomics and metatranscriptomics. Cellulose acetate (CA), polybutylene succinate (PBS), and polyhydroxybutyrate (PHB) degraded at varying rates across materials, seasons, and experimental settings, with up to 28% weight attrition after 97 weeks *in situ* (CA) and 56% carbon loss to CO_2 after four weeks *in vitro* (PBS). The three biodegradable plastics developed similar microbial communities with lower richness and different composition from those on the non-biodegradable materials (polyamide, polyethylene, and glass) and in the water column. The microbial populations on the biodegradable plastics included mostly aerobic and facultative anaerobic heterotrophs with a broad carbohydrate metabolism, and with a higher prevalence of denitrification and other nitrogen cycling traits compared to the non-biodegradable materials. Based on the metatranscriptomic signal of key genes involved in CA, PBS, and PHB breakdown, we identified diverse microbial populations that can potentially drive the biodegradation of these materials in the Baltic Sea, many of which encoded the potential to degrade multiple bioplastics. We propose the term *bioplastisphere* to denote the specialised microbial communities associated with biodegradable plastics.

Key words: Baltic Sea, plastisphere, metagenomics, metatranscriptomics.

Introduction

Millions of tonnes of plastics enter the oceans each year, making plastic pollution one of the most pressing environmental challenges of our time [1–3]. Plastics accumulate in coastal regions, surface waters, and sediments, where they can cause long-lasting environmental harm [4–6]. The amount of mismanaged plastic waste in the environment is projected to triple in the coming decades due to increasing industrial and societal demands combined with inadequate waste management practices [7].

Conventional fossil fuel-based plastics, particularly polyethylene, dominate the plastic industry due to their high durability against biotic and abiotic degradation, which also makes them the main constituents of marine plastic pollution [1, 8, 9]. Bioplastics—*i.e.* plastics that are biodegradable or produced from renewable, bio-based sources—are increasingly popular as part of a wider strategy to reduce both environmental pollution and the use of finite fossil fuel resources [10]. However, many bioplastic materials only achieve full degradation under tightly constrained conditions, such as those certified by the EU standard EN13432 for industrial composting [11]. Plastic biodegradation is much slower in the marine environment, which is generally colder, more oligotrophic, and contains lower microbial biomass and diversity than compost and soil [12]. Because both material properties and environmental conditions influence plastic biodegradation, there is little consensus about the general biodegradability of different bioplastic materials [13, 14]. Current industrial directives do not address adequately the impact of mismanaged bioplastic waste on the marine environment, which remain poorly understood.

Plastics can serve as a substrate for microbial growth and biofilm formation in marine environments and microorganisms are the main drivers of plastic biodegradation [15–17]. Microorganisms colonise marine plastics readily and the communities are considered mature in the order of one month [18–21]. The community composition of the plastisphere—*i.e.* the ecosystem comprising plastic debris and associated microorganisms—is driven by biogeographical and environmental factors [22–26], but the importance of material properties is still under debate [20, 27, 28]. Increasing evidence suggests that the microbial communities colonising some bioplastic materials (*e.g.* polyhydroxybutyrate and cellulose acetate) are different and more active than those on conventional plastics, whereas the communities on non-biodegradable bio-based plastics (*e.g.* polylactic acid) resemble those on conventional plastics [19, 28–31]. In general, the communities on both bio- and fossil fuel-based plastics are dominated by Alpha- and Gammaproteobacteria [22, 25, 28], which appear to correlate with the loss of material or observed biodegradation of certain bioplastics [19, 29, 31]. Despite considerable advances in recent years, our knowledge of marine plastic biodegradation and associated microbial communities contains significant gaps, including not only the microbial pathways involved in the breakdown of different bioplastics but also their connections with the marine carbon and nitrogen cycles.

Common approaches to investigate plastic biodegradation have included measuring plastic weight attrition and changes in chemical and mechanical properties [32], respirometry [33], isotopic labelling [34], microbial community analyses [35], and combinations of all of these [31, 36–38]. Most studies have applied controlled *in vitro* experiments that do not reflect the complex, variable conditions of marine environments,

and so extrapolation to the natural environment is often difficult. Long-term *in situ* investigations are rare, particularly studies combining biodegradation measurements and microbial community analyses [39–43]. Recent studies have shown that metagenomics is a powerful tool to investigate the functional potential of microbial communities and their role not only in plastic biodegradation but also other biogeochemical processes [28, 44–47]. For example, Fortin *et al.* [28] reported increased denitrification potential as communities mature during the first months of plastic colonization in a coastal estuary. This study also showed that genes for nitrogen metabolism are typically present in many common plastisphere taxa such as Alpha- (*e.g.* Rhizobiales and Rhodobacterales) and Gammaproteobacteria (*e.g.* Burkholderiales and Pseudomonadales).

Central to a more accurate understanding of marine plastics is considering biodegradation as a systemic capacity, *i.e.* by investigating the microbial communities and the environmental conditions constraining their activity. Here, we assessed the biodegradation of six bio-based bioplastic materials in the brackish Baltic Sea under multi-seasonal *in situ* and *in vitro* conditions. Coupling measurements of plastic weight attrition, spectroscopy, respirometry, metagenomics, and metatranscriptomics, we investigated differences in biodegradation between the materials throughout different seasons and explored the links between biodegradation and microbial community composition. We hypothesise that community composition—including the presence and activity of plastic-degrading genes—is structured by the physicochemical properties of the bioplastics and therefore unique to each material.

Materials and Methods

Experimental setup

Bioplastic materials. We investigated six types of bio-based bioplastics, which will be designated from now on simply as bioplastics: cellulose acetate (CA), cellulose acetate propionate (CAP), polybutylene succinate (PBS), polyhydroxybutyrate/valerate (PHB), polyamide (PA), and polyethylene (PE). Injection-moulded bioplastic sheets were provided by VTT Technical Research Centre of Finland (Espoo, Finland).

***In situ* mesocosm.** The mesocosm experiment was set up in July 2021 at the Tvärminne Zoological Station, University of Helsinki (Hanko, Finland, 59.845°N, 23.250°E). The salinity of the Baltic Sea in the study area is 5–6 and the water temperature during the experiment ranged from +2.5°C to +25.0°C. Sixty bioplastic sheets (15 mm width × 100 mm length × 3 mm thickness) of each material were individually weighted, secured to racks, and transferred to a 400 l flow-through tank connected to the Baltic Sea. Glass sheets of identical dimensions were included as control. The mesocosm environment was kept in the dark to prevent the growth of photosynthetic microeukaryotes. At six sampling times (September 2021, January, March, and August 2022, and January and May 2023), five sheets of each material were sampled for biodegradation measurements and five for molecular analyses (metagenomics and metatranscriptomics). Five seawater samples (1000 ml) were also taken from inside the mesocosm tank for the molecular characterization of the planktonic communities, and three seawater samples (250 ml) were taken to be used as inoculum in the *in vitro* experiments. The bioplastic samples for

127 biodegradation measurements were kept at –20°C until processing, and the samples for
128 the molecular and *in vitro* analyses were processed immediately.

129 ***In vitro* experiments.** For each bioplastic material and the seven sampling times
130 indicated above (July 2021–May 2023), 0.25 g l^{-1} of milled bioplastic was added to three
131 amber-coloured 600 ml bottles containing 250 ml of seawater collected from the mesocosm
132 tank. The bioplastic materials were frozen in liquid nitrogen to decrease their tensile
133 strength and finely milled (< 0.3 mm particle size) with a rotary-blade mill. To prevent
134 nutrient limitation during the experiment, 0.1 g l^{-1} KH_2PO_4 and 0.5 g l^{-1} NH_4Cl were
135 added. Microcrystalline cellulose (MCC) with an average particle size of 90 µm (Xylem
136 Analytics, Weilheim, Germany) was used as positive control, and negative controls
137 without bioplastic were also included. The bottles were incubated with mild agitation in
138 the dark at 15°C for 28 days and then processed immediately.

139 Biodegradation measurements

140 Bioplastic biodegradation in the *in situ* mesocosm was estimated based on weight attrition
141 and changes in the surface chemical structure were assessed using Fourier transform
142 infrared (FTIR) spectroscopy. The bioplastic sheets were immersed in 2% sodium dodecyl
143 sulphate (SDS) and kept overnight at 35°C with mild agitation, then brushed gently,
144 rinsed with ultrapure water, and dried overnight at room temperature. The sheets were
145 weighted with an EP-225-SM-DR balance (Precisa Gravimetrics AG, Dietikon,
146 Switzerland), and weight attrition was calculated as the difference between the initial
147 and post-incubation weights divided by the initial weight. FTIR spectroscopy analysis of
148 the bioplastic sheets was done using the Agilent 4300 device (Agilent, Santa Clara, USA)
149 in the spectral range of 650–4000 cm^{-1}, and the data was analysed with *MicroLab* v5.8
150 [48]. The obtained spectra were compared to reference data from the Polymers and
151 Polymer Additives Spectra Database P/N 30002, and changes in surface structure were
152 calculated as the difference between the initial and post-incubation spectra.

153 *In vitro* bioplastic biodegradation was estimated according to the D6691-17 standard [33]
154 using a WTW OxiTop-IDS12 respirometer (Xylem Analytics, Weilheim, Germany), which
155 records biological oxygen demand (BOD) by pressure difference from the absorption of
156 CO_2 evolved during incubation with NaOH. BOD was converted to carbon loss to CO_2
157 based on carbon contents determined using a CHN analyser (ALS, Prague, Czechia).

158 Metagenome and metatranscriptome sequencing

159 For molecular analyses, the *in situ* bioplastic sheets were scraped using a sterile scalpel
160 and the biofilm was transferred to a 2 ml Lysing Matrix E tube (MP Biomedicals, Irvine,
161 USA). The *in situ* seawater and the *in vitro* samples were vacuum filtered on a Whatman
162 0.22 µm membrane (Cytiva, Marlborough, USA) and transferred to a 2ml cryovial. The
163 tubes were flash frozen in liquid nitrogen and stored at –80°C until extraction. DNA and
164 RNA was extracted using a cetrimonium bromide (CTAB), phenol-chloroform, and bead-
165 beating protocol modified from Viitamäki *et al.* [49]. After bead-betting, the extract was
166 transferred to a clean tube and centrifuged at 16,000 × g for 5 min at 4° C. The aqueous
167 top layer was transferred to a clean tube containing 500 µl of ≥ 99.9% stabilised
168 chlorophorm (VWR Chemicals, Radnor, USA), and the extraction continued as further
169 described [49]. Blank samples were extracted and sequenced in parallel.

Library preparation and sequencing were done at the DNA Sequencing and Genomics Laboratory (University of Helsinki, Helsinki, Finland). The DNAprep kit (Illumina, San Diego, USA) with in-house Nextera primers was used for the metagenomic analyses and the NEBNext Ultra II Directional RNA kit (New England Biolabs, Ipswich, USA) for metatranscriptomics. Sequencing was done with the Illumina NovaSeq 6000 system using the S4 chemistry (2 × 150bp). In total, 391 metagenomes and 78 metatranscriptomes were sequenced, yielding 1.5 Tb and 508.6 Gb with a median output of 3.4 Gbp and 6.9 Gbp per sample, respectively (**Table S1**). Some PA, PE, and glass metagenomes and metatranscriptomes yielded very few reads, and several samples could not be sequenced due to low RNA yield. *Cutadapt* v4.4 [50] was used to trim sequencing adapters, low quality base calls (Phred score < 28), and poly-A tails, and to discard short reads (< 50 bp after trimming) and reads containing ambiguous base calls. The quality of the raw and filtered data was assessed with *FastQC* v0.12.1 [51] and *MultiQC* v1.15 [52].

Taxonomic profiling

The metagenomic and metatranscriptomic reads were classified at the domain level using *Kaiju* v1.10.0 and the *nr_euk* database release 2023-05-10 [53]. A more detailed taxonomic profiling of bacteria and archaea was obtained based on 59 single-copy marker genes with *SingleM* v0.16.0 [54]. For each gene, the metagenomic reads were screened for a conserved 60-bp window using a hidden Markov model (HMM). The matching sequences were extracted, clustered by exact sequence matching and classified based on reference protein sequences from the Genome Taxonomy Database (GTDB) release 214 [55]. A consensus taxonomic profile was then obtained by summarizing the coverage of each taxon across the 59 marker genes, which was then standardised to relative abundance.

Genome-resolved metagenomics

The metagenomes were assembled and binned using the *snakemake* metagenomics workflow in *anvi'o* v7.1 [56]. For each group of 3–5 replicates, the filtered reads were pooled and assembled using *MEGAHIT* v1.2.9 [57] with a minimum contig length of 1000 bp, and gene calls were identified with *Prodigal* v2.6.3 [58]. Taxonomy was assigned to the contigs based on a set of 71 bacterial and 76 archaeal single-copy genes [59] identified with *HMMER* v.3.3.2 [60] and classified with *DIAMOND* v2.1.7 [61] against the GTDB release 89 [55]. The metagenomic reads were mapped to the contigs with *Bowtie2* v2.3.5 [62] and *SAMtools* v1.10 [63], and *MetaBAT2* v2.15 [64] was used to bin metagenome-assembled genomes (MAGs) based on tetranucleotide frequency and differential coverage. The MAGs from all the different assemblies were pooled and pairwise average nucleotide identity (ANI) values were computed with *FastANI* v1.3.2 [65]. For each cluster of MAGs with ≥ 98% ANI, a representative MAG with the highest score was selected, where:

$$score = completion - (2 \times redundancy) + (\log(N_{50}) / 2) + (\log(length) / 2)$$ (modified from [66]).

The non-redundant MAGs were visually inspected using *anvi'o* v8.0 [56] and contigs with discrepant coverage, tetranucleotide frequency, or taxonomic signal were removed. The MAGs were classified against the GTDB release 214 [55] with *GTDB-Tk* v2.3.0 [67].

The metagenomic and metatranscriptomic reads were mapped to the curated non-redundant MAGs with *Bowtie2* v2.5.1 [62] and *SAMtools* v1.18 [63], and *CoverM* v0.7.0 [68] was used to summarise the number of reads recruited by each MAG. Only matching

213 reads with ≥ 95% sequence identity and ≥ 75% coverage and MAG-level horizontal
214 coverage ≥ 10% were considered, and abundances were normalised to reads per kilobase
215 per million mapped reads (RPKM). Gene-level coverage and detection in the
216 metatranscriptomes were obtained with *anvi'o* v8.0 [56]. Putative plastic-degrading genes
217 were annotated by searching the gene calls against the KOfam [69] and CAZy [70]
218 databases with *HMMER* v.3.3.2 [60] in *anvi'o* v8.0 [56] (e-value < 10^{-12}), and the PlasticDB
219 database [71] with *DIAMOND* v2.1.8 [61] (≥ 30% amino acid similarity and ≥ 70%
220 alignment). MAG-level reconstruction of metabolic traits was obtained with *microTrait*
221 v1.0.0 [72]. Trait prevalence was calculated as the proportion of MAGs containing the
222 trait relative to all the MAGs with horizontal coverage ≥ 25% in a given sample.

223 ## Statistical analyses

224 Statistical analyses were done in *R* v4.3.3 [73]. Significant differences in biodegradation
225 and *rpsB* richness between the materials were assessed using analysis of variance
226 (ANOVA) followed by the Sidak test using the packages *stats* v4.3.3 [73], *emmeans* v1.10.6
227 [74], and *multcomp* v1.4.26 [75]. The richness of *rpsB* variants was estimated after
228 subsampling the dataset to 325 *rpsB* reads per sample. The *rpsB* read counts were
229 standardised using the Hellinger transformation, pairwise Bray-Curtis dissimilarities
230 were computed, and differences in community structure were assessed by Principal
231 coordinates analysis (PCoA) and permutational multivariate ANOVA (PERMANOVA)
232 using the package *vegan* v2.7.1 [76]. Differentially abundant genera, traits, and MAGs
233 were identified using linear regression with the package *Maaslin2* v1.16.0 [77]. The data
234 was log-transformed prior to model fitting, and the *p*-values were adjusted using the
235 Benjamini-Hochberg false discovery rate (FDR).

236 # Results

237 ## *In situ* and *in vitro* bioplastic biodegradation

238 Biofilms were visible on the CA, PBS, and PHB sheets already at the second sampling
239 time, 12 weeks after the start of the mesocosm experiment (**Fig. S1a**). CA and PBS, in
240 particular, developed thick, slimy biofilms with pronounced black pigmentation. Biofilm
241 development was less pronounced on the other bioplastic materials (CAP, PA, and PE)
242 and glass, which was used as the biofilm control. *In situ* biodegradation rates based on
243 weight attrition differed significantly between the bioplastic materials (ANOVA,
244 $R^2 = 0.99$, $p < 0.001$) (**Fig. 1a**). CA degraded the most (27.8% ± 0.2% weight attrition after
245 97 weeks) followed by PBS (12.7% ± 1.0%) and PHB (7.1% ± 0.2%). Weight attrition was
246 negligible for CAP (1.3% ± 0.2%) and below detection for PA and PE. A comparable pattern
247 was observed with FTIR spectroscopy, which revealed pronounced changes in the surface
248 chemical structure of the CA, PBS, and PHB sheets but not CAP, PA, and PE (**Fig. S1b**).

249 I*n vitro* biodegradation rates also varied significantly between the materials (ANOVA,
250 $R^2 = 0.71$, $p < 0.001$) (**Fig. S2a**). PBS degraded the most (56.0% ± 7.2% carbon loss to CO_2
251 after four weeks) followed by CA (32.8% ± 2.2%) and PHB (26.8% ± 11.5%). Negligible
252 carbon loss was measured for PA and PE (1.8% ± 1.4% and 1.1% ± 1.0%, respectively),
253 likely reflecting the utilisation of residual plastic additives. The *in vitro* biodegradation of
254 CAP was not assessed. Temporal differences in biodegradation were observed for some
255 materials (ANOVA, $R^2 = 0.76–0.99$, $p < 0.001$) (**Fig. S2b**). Whereas CA had uniform

biodegradation, PBS varied from 7.0 ± 0.0% to 62.7% ± 4.7% and PHB from 10.7% ± 0.6% to 44.3% ± 5.0%. PBS and PHB had the highest biodegradation for communities sampled in winter (January 2022 and 2023, respectively). CA, PBS, and PHB degraded in both *in situ* and *in vitro* conditions and will be hereafter designated as biodegradable plastics.

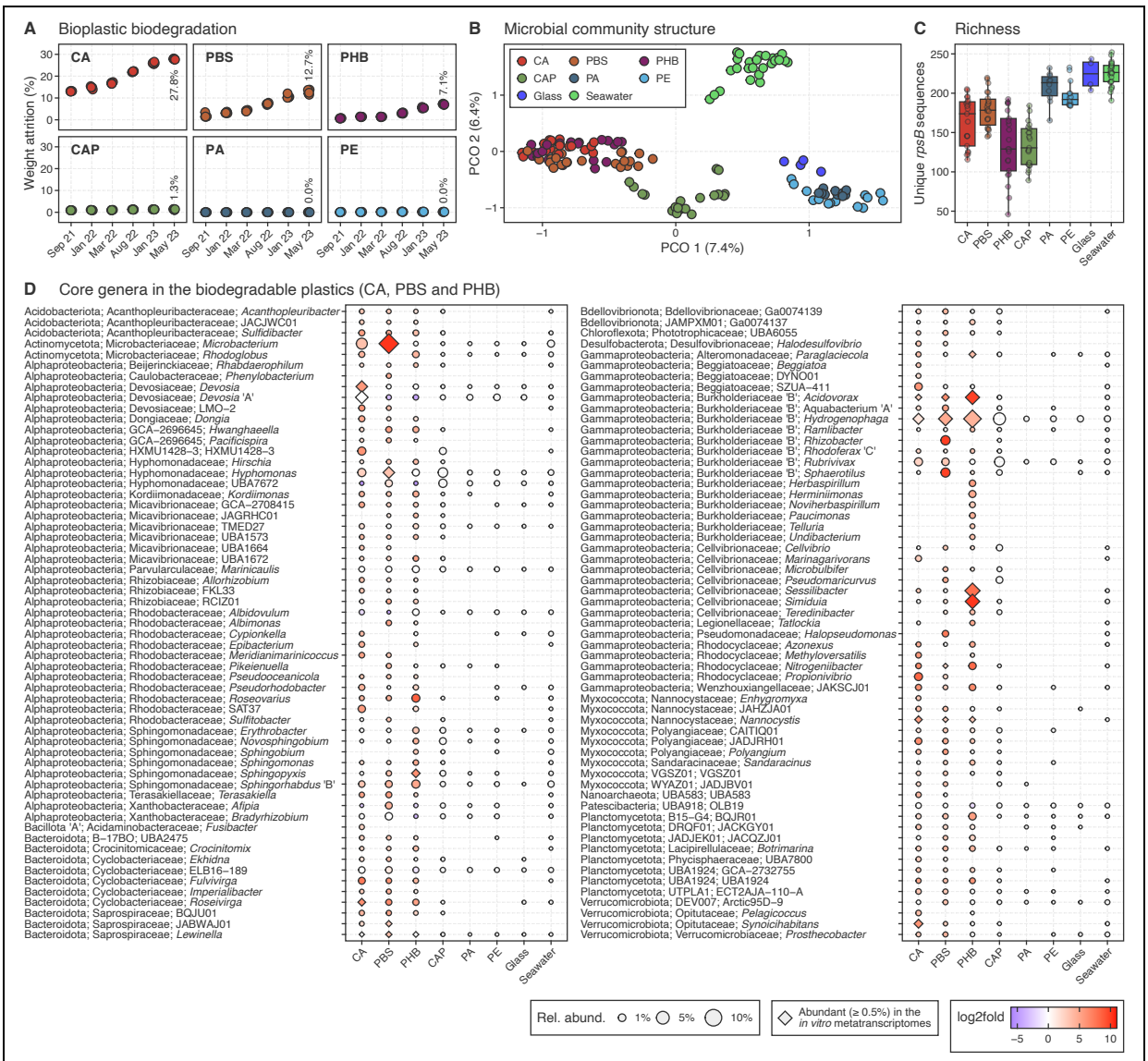

Figure 1. Bioplastic biodegradation and associated microbial communities during a 97-week *in situ* mesocosm experiment in the Baltic Sea. a) Biodegradation rates of six bio-based bioplastic materials based on weight attrition relative to the start of the experiment (July 2021). **b)** Microbial community structure based on unique 60-bp *rpsB* sequences extracted from the metagenomic reads. Principal coordinates analysis (PCoA) of Bray-Curtis distances of Hellinger-transformed counts. **c)** Microbial richness based on unique 60-bp *rpsB* sequences, calculated after subsampling to even depth. **d)** Abundance of core genera in the biodegradable plastics (CA, PBS, and PHB), defined as those with ≥ 0.5% relative abundance or that were significantly more abundant in these materials compared to the inert surfaces (PA, PE, and glass) according to linear regression (log2fold ≥ 3.0, adjusted $p < 0.05$). Consensus taxonomic profile based on 59 marker gene sequences extracted from the metagenomic reads (60-bp fragments). Relative abundance is shown as the 10% trimmed mean across five biological replicates and six sampling times. Genera shown with a diamond had ≥ 0.5% relative abundance in the associated *in vitro* metatranscriptomes (**Fig. S7**). In **b** and **c**, samples with < 325 *rpsB* reads were not included.

Microbial communities associated with the bioplastics

Analysis of reads matching the *rpsB* gene (ribosomal protein S2) of archaea and bacteria showed that the *in situ* metagenomes were significantly structured by material (PERMANOVA, $R^2 = 0.26$, $p < 0.001$). The PCoA clustered the metagenomes into four groups comprising *i)* the three biodegradable plastics (CA, PBS, and PHB); *ii*) the slowly degrading bioplastic (CAP); *iii*) the inert surfaces, including the bioplastics that did not degrade (PA and PE) and the biofilm control (glass); and *iv*) the planktic seawater metagenomes (**Fig. 1b**). The metagenomes from the biodegradable plastics and CAP had significantly lower *rpsB* richness than the other two groups (ANOVA, $R^2 = 0.63$, $p < 0.001$) (**Fig. 1c**). The metagenomes were also temporally structured (PERMANOVA, $R^2 = 0.09$–0.22, $p < 0.001$). The temporal dynamics varied between the biofilm and planktic datasets, with the biofilm metagenomes from both the biodegradable and non-biodegradable plastics diverging linearly over time, while the planktic seawater metagenomes followed a more pronounced seasonal dynamic (**Fig. S3**). In general, the metagenomes had homogeneous *rpsB* structure between the biological replicates (**Fig. S4**). Consistent *rpsB* structure was observed for the biodegradable plastics across the *in situ* and *in vitro* metagenomes and metatranscriptomes (**Fig. S5**), which suggests that we were able to capture an active microbial community that is likely linked to the biodegradation of these materials. On the other hand, the *in situ* PA and PE metagenomes clustered with the glass metagenomes, whereas the *in vitro* PA and PE metagenomes were similar to the seawater metagenomes and metatranscriptomes, suggesting activity not related to the substrate.

Potential microbial drivers of bioplastic biodegradation

Comparison with sequences from the GenBank *nr* database revealed that bacteria comprised a large fraction (98.0% ± 0.2% of the reads) of the metagenomes (**Fig. S6**). Both *in situ* and *in vitro* experiments were done in the dark to focus on heterotrophic biodegradation and so the metagenomes contained a very low proportion of photosynthetic microeukaryotes, which are usually abundant members of the plastisphere [27, 44]. The *in situ* bioplastic metagenomes were dominated by members of the Gamma- (26.8% ± 1.2% of the reads) and Alphaproteobacteria (22.6% ± 0.6%), followed by Planctomycetota (9.6% ± 0.4%), Actinomycetota (8.9% ± 0.7%), Bacteroidota (5.2% ± 0.2%), Myxococcota (2.8% ± 0.2%), Acidobacteriota (1.8% ± 0.1%), and Verrucomicrobiota (1.3% ± 0.2%) (**Fig. S7**). When considering the abundant genera—defined as those representing ≥ 0.5% of the reads in each material—only a small number of taxa were shared between the biodegradable plastic metagenomes and the other groups, and the three biodegradable plastics collectively contained the largest fraction of the total generic diversity (**Fig. S8**). Community composition in the *in vitro* metagenomes was generally comparable to the *in situ* metagenomes (**Fig. S7**).

To explore the microorganisms that might be driving bioplastic biodegradation, we analysed in more detail the core genera in the biodegradable plastic metagenomes. These consisted of 118 microbial genera that were represented by ≥ 0.5% of the reads in the CA, PBS, and PHB *in situ* metagenomes, or that were significantly more abundant in these materials compared to the inert surfaces (linear regression, log2fold ≥ 3.0, adjusted $p < 0.05$). Many core genera were shared between the different biodegradable plastics

318 (**Fig. 1d**). For example, *Microbacterium* (Microbacteraceae, Actinomycetota) was the most
319 abundant genus in the PBS and CA metagenomes (8.6% ± 1.0% and 3.2% ± 1.4% of the
320 reads, respectively). *Hydrogenophaga* (Burkholderiaceae 'B', Gammaproteobacteria),
321 which was the most abundant genus in PHB (6.6% ± 1.1%), was also abundant in PBS
322 (3.4% ± 0.4%) and CA (1.6% ± 0.7%). Other core genera that were shared between the
323 biodegradable plastics included *Hyphomonas* (Hyphomonadaceae, Alphaproteobacteria),
324 *Sphingorhabdus* 'B' (Sphingomonadaceae, Alphaproteobacteria), *Acidovorax*
325 (Burkholderiaceae 'B', Gammaproteobacteria), *Fulvivirga*, and *Roseivirga* (both
326 Cyclobacteriaceae, Bacteroidota), and *Nannocystis* (Nannocystaceae, Myxococcota),
327 among others (**Fig. 1d**). Many core genera in the *in situ* metagenomes were also abundant
328 *in vitro*, including in the metatranscriptomic space, indicating a putative function in
329 biodegradation given that bioplastic was the sole carbon source in these controlled
330 experiments (**Fig. 1d, Fig. S7**).

331 Microbial traits associated with the bioplastics

332 We assembled and binned the metagenomes to investigate in more detail the phylogenetic
333 and functional composition of the microbial populations associated with the bioplastics.
334 Binning yielded 5,129 non-redundant MAGs (≥ 98% ANI) which represented a substantial
335 fraction of the metagenomes, recruiting 45.4% ± 19.4% of the reads and reaching up to
336 70% in some samples (**Table S1**). In addition, the phylogenetic placement of the MAGs
337 (**Fig. S9**) was consistent with the taxonomic profiles inferred from the reads (**Fig. S7**),
338 further indicating that the genome-resolved approach captured well the metagenomic
339 diversity. Metabolic reconstruction showed that the functional composition of the *in situ*
340 metagenomes was also structured by material (PERMANOVA, $R^2 = 0.48$, $p < 0.001$), with
341 a clear separation between the biodegradable, non-biodegradable, and seawater
342 metagenomes (**Fig. S10**). Differently to the results based on the *rpsB* gene, the CAP
343 metagenomes clustered with the biodegradable plastics in the trait-based analysis.

344 We searched the MAGs for key genes involved in the initial hydrolysis of CA, PBS, and
345 PHB to track the microbial populations that are potentially driving the biodegradation of
346 these materials. The prevalence of bioplastic-degrading traits—defined as the proportion
347 of MAGs containing the trait in a given sample—was generally higher in the *in situ*
348 biodegradable plastic metagenomes compared to the inert surfaces (linear regression,
349 adjusted $p < 0.05$) (**Fig. 2**, **Fig. S11**). Genes encoding carbohydrate esterases (CAZy
350 families CE1 and CE2) and glycoside hydrolases (CAZy families GH5, GH9, GH45, and
351 GH48), which function in CA deacetylation and hydrolysis, respectively, were identified
352 in 11.0% ± 0.4% of the MAGs detected in the biodegradable plastics. Genes functioning in
353 PBS hydrolysis were identified in 11.7% ± 0.3% of the MAGs (**Fig. 2**, **Fig. S11**), and most
354 were related (≥ 30% amino acid similarity and ≥ 70% alignment) to a PLA depolymerase
355 derived from an uncultured microorganism with verified enzymatic activity against PBS
356 [78]. Finally, genes encoding PHB depolymerases were identified in 40.7% ± 0.6% of the
357 MAGs from the biodegradable plastics, 21.1% ± 2.8% from the inert surfaces and 14.3% ±
358 0.8 from the seawater metagenomes (**Fig. 2**, **Fig. S11**).

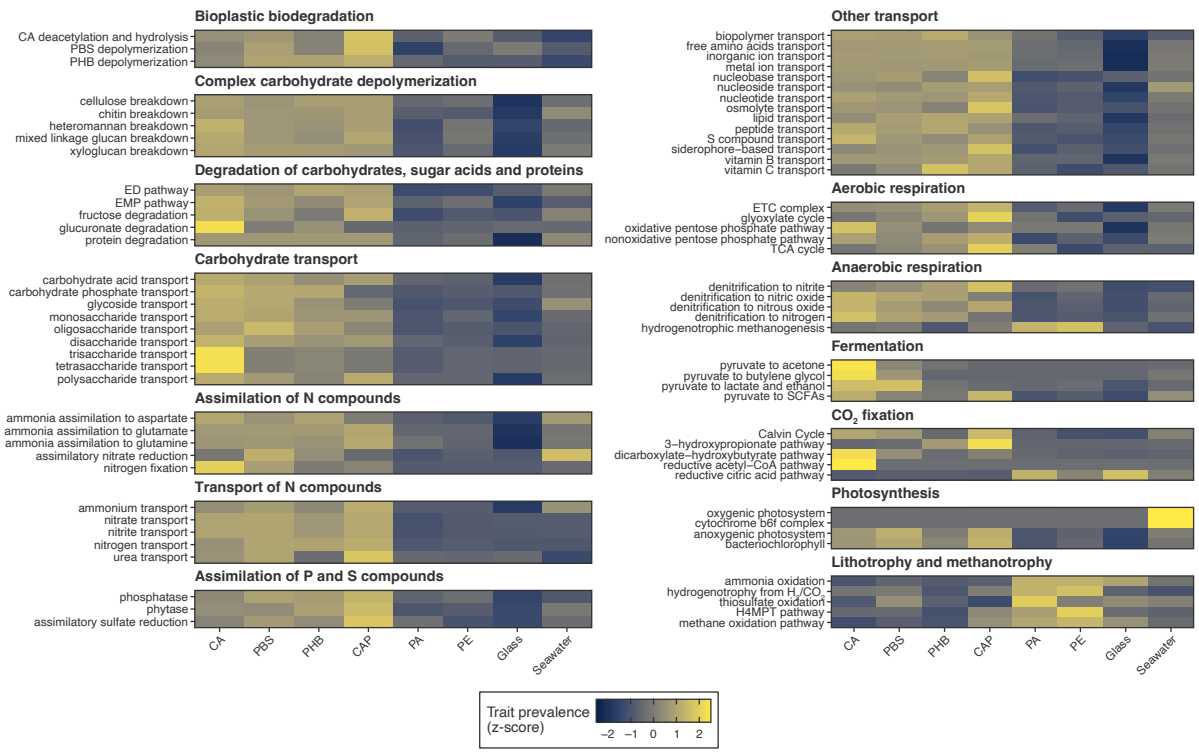

Figure 2. Microbial traits associated with bioplastic biodegradation in the *in situ* mesocosm. Trait prevalence represents the proportion of metagenome-assembled genomes (MAGs) containing the trait relative to all the MAGs detected in a given sample (≥ 25% horizontal coverage). Trait prevalence is shown as the 10% trimmed mean across five biological replicates and six sampling times followed by trait-wise z-score standardisation.

Other metabolic traits were also more prevalent in the *in situ* biodegradable plastic metagenomes compared to the inert surfaces (linear regression, adjusted $p < 0.05$) (**Fig. 2**, **Fig. S11**). These included traits related to carbohydrate depolymerization, degradation, and transport (notably the breakdown of cellulose and chitin and the transport of mono- and disaccharides), the assimilation and transport of nitrogen, phosphorus, and sulphur compounds (notably nitrogen fixation and nitrate, nitrite, and nitrogen transport), aerobic respiration, anaerobic respiration (mainly denitrification), pyruvate fermentation, CO_2 fixation (mainly via the Calvin cycle), and anoxygenic photosynthesis. On the other hand, lithotrophic traits (notably ammonia oxidation, hydrogenotrophy, and thiosulfate oxidation), methane oxidation, and hydrogenotrophic methanogenesis were more prevalent in the non-biodegradable plastic and glass metagenomes (**Fig. 2**, **Fig. S11**).

Microbial populations in the biodegradable plastics

We investigated bioplastic biodegradation in more detail by analysing the core microbial populations in the biodegradable plastics. These consisted of 227 medium to high quality MAGs (79.3% ± 2.1% complete, 2.8% ± 0.3% redundant) that recruited ≥ 0.5% of the reads in the CA, PBS, and PHB *in vitro* and *in situ* metagenomes and metatranscriptomes, or that were significantly more abundant in these compared to the inert materials (linear regression, log2fold ≥ 3.0, adjusted $p < 0.05$) (**Table S2**). The potential for CA, PBS, and PHB biodegradation was detected in 14.5%, 18.9%, and 61.7% of the core MAGs, respectively, and 19.8% encoded the potential to degrade two or more bioplastics (**Fig.**

384 **3a**). Most core MAGs with plastic-degrading traits belonged to Alpha- and
385 Gammaproteobacteria, Actinomycetota, Bacteroidota, and Myxococcota (**Fig. 3b**).

386 The *in vitro* metatranscriptomes enabled us to probe the activity of specific genes and
387 identify microbial populations that are likely involved in bioplastic biodegradation. Since
388 bioplastic was the only carbon source in the *in vitro* experiments, the metatranscriptomic
389 signal of key genes involved in CA, PBS, and PHB hydrolysis can be seen as a strong
390 indication of microbial populations that are actively participating in the biodegradation
391 of these materials. Metatranscriptomic activity was observed for 36.3%, 16.3% and 42.9%
392 of the MAGs carrying the genes for CA, PBS, and PHB hydrolysis, respectively (**Fig. 3c**).
393 The two Nannocystaceae MAGs (Myxococcota) encoded the potential to degrade the three
394 biodegradable plastics, but the gene for PBS hydrolysis was not active in both MAGs. The
395 *Simiduia* MAGs (Gammaproteobacteria) had active genes for CA and PHB degradation,
396 and the *Acidovorax* and *Hydrogenophaga* MAGs (both Gammaproteobacteria) showed
397 metatranscriptomic activity for PHB and PBS degradation. In general, the taxonomy of
398 the MAGs with active CA, PBS, and PHB genes matched many of the core genera in the
399 biodegradable plastics identified from the metagenomic reads (**Fig. 1d**, **Fig. S7**).

400 Metabolic reconstruction suggested that the MAGs with active CA, PBS, and PHB genes
401 comprised mostly aerobic heterotrophs with broad carbohydrate-degrading capabilities,
402 including the breakdown of cellulose, chitin, heteromannan, mixed lineage glucan, and
403 xyloglucan (**Fig. 3c**). In addition to aerobic respiration, many Alpha- and
404 Gammaproteobacteria MAGs with active PBS and PHB genes also encoded the potential
405 for anaerobic respiration via complete and truncated (to nitrite, nitric oxide, or nitrous
406 oxide) denitrification, CO_2 fixation (mostly via the Calvin cycle), anoxygenic
407 photosynthesis, and nitrogen fixation. Many MAGs also encoded the potential for
408 thiosulfate oxidation, indicating a flexible organo- and lithotrophic metabolism.

409 Discussion

410 Our combined experimental approach, which included metagenomic and
411 metatranscriptomic data from multi-seasonal *in situ* and *in vitro* experiments, enabled a
412 detailed characterisation of the biodegradation of different bioplastics in the Baltic Sea.
413 We observed variable biodegradation rates across materials, seasons, and experimental
414 settings. CA, PBS, and PHB degraded 7–28% after 97 weeks *in situ* and 27–56% after four
415 weeks *in vitro*, and CAP, PA, and PE had low to negligible biodegradation in both settings.
416 In all, the biodegradation rates observed *in situ* were much lower than what is required
417 by current industrial standards regulating bioplastic labelling, which only consider
418 biodegradation under optimal conditions such as industrial composting [11]. The high
419 degradation of PBS is in contrast with previous studies in marine and freshwater
420 environments [29], and only the biodegradation of low molecular weight PBS has been
421 previously observed in seawater [79]. The higher *in vitro* biodegradation rates compared
422 to *in situ* might be attributed to experimental differences in material geometry (< 0.3 mm
423 particles were used *in vitro* and 3 mm-thick sheets *in situ*), since smaller plastic particles
424 are generally easier to degrade [31, 80]. In addition, the variable biodegradation rates in
425 the *in vitro* experiments, which were done under controlled environmental settings,
426 suggest that the biodegradation potential of the Baltic Sea microbial communities
427 fluctuates across seasons and years. Seasonal variation in biodegradation potential [31]

and microbial community structure [22, 23] has been observed in previous studies. Altogether, these results suggest that the effects of environmental, material geometry, and inoculum composition should be considered when assessing marine bioplastic biodegradation.

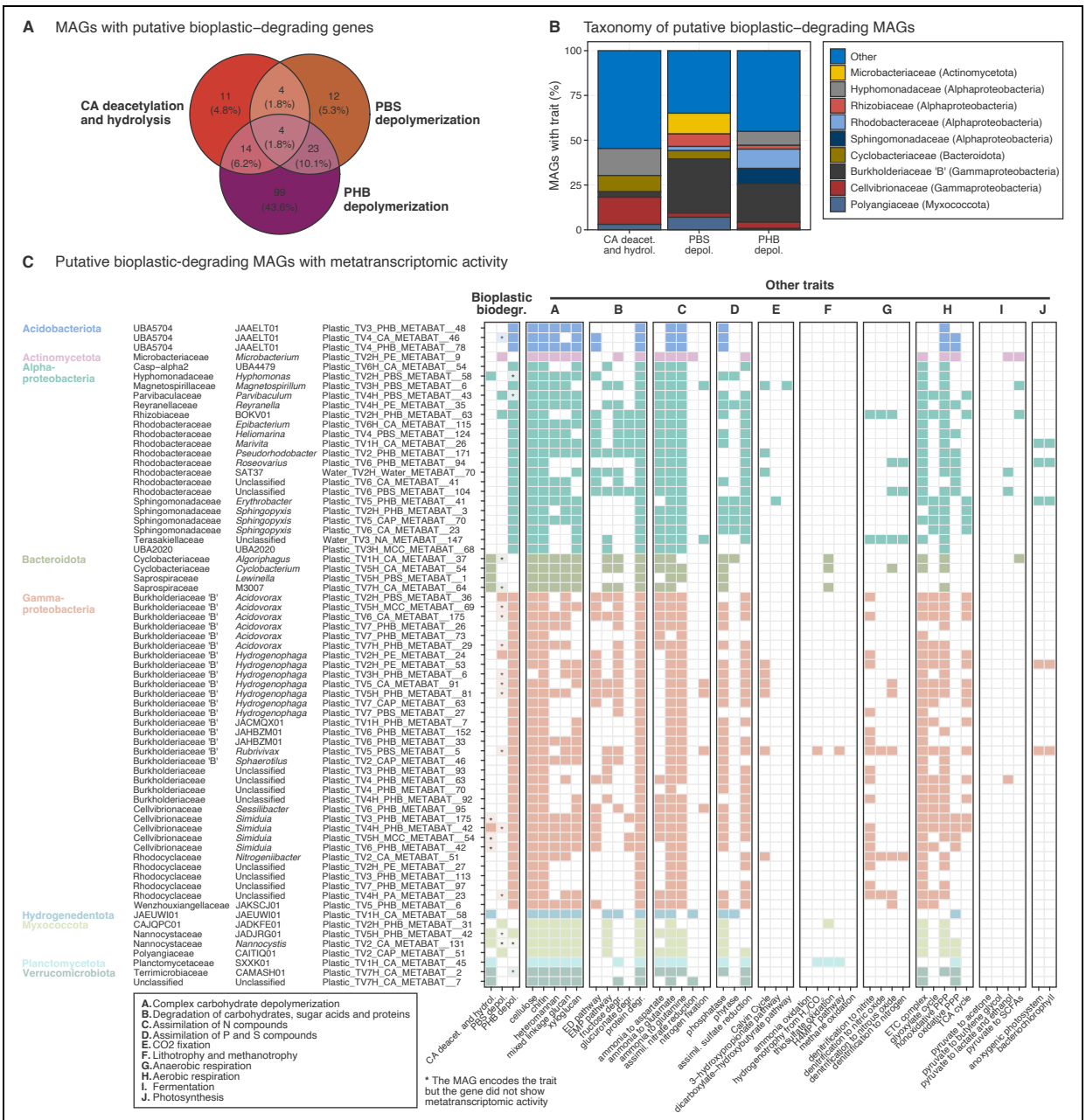

Figure 3. Microbial populations from the Baltic Sea with putative function in bioplastic biodegradation. Core microbial populations defined as those with ≥ 0.5% relative abundance in the CA, PBS, and PHB *in situ* and *in vitro* metagenomes and metatranscriptomes, or that were significantly more abundant in these compared to the inert materials (PA, PE, and glass) according to linear regression (log2fold ≥ 3.0, adjusted $p < 0.05$). **a)** Metagenome-assembled genomes (MAGs) with putative plastic-degrading genes, **b)** their family-level taxonomic classification, and **c)** detailed information on MAGs that showed gene activity in the *in vitro* metatranscriptomes. Percentages in **a** are relative to the total number of core MAGs ($n = 227$).

In line with our hypothesis, microbial community structure and richness differed between the bioplastics in both taxonomic and functional spaces, and a clear distinction was observed between the biodegradable and non-biodegradable plastics. The clustering of PA and PE with glass agrees with other studies and suggests that non-biodegradable plastics act mainly as a substrate for biofilm development in the marine environment, having little effect on community composition [20, 25, 27, 81]. The separation between biodegradable and non-biodegradable plastics agrees with previous observations of distinct microbial community and higher cell specific activities in biodegradable CA and PHB compared to non-biodegradable materials [19, 31, 81], whereas PBS seems to be more resistant to biodegradation in the marine environment [29]. In all, our long-term, multi-seasonal study shows that, whereas conventional plastics and inert surfaces seem to harbour similar microbial communities despite differences in physicochemical properties, distinct biodegradable plastics can indeed support taxonomically and functionally convergent microbial communities. We refer to the specialised microbial community of biodegradable plastics as the *bioplastisphere*.

Our genome-resolved analysis evidenced a widespread potential for CA, PBS, and PHB hydrolysis across the bioplastisphere independently of substrate, with many abundant populations harbouring the potential to degrade multiple bioplastics. Importantly, the metatranscriptomic activity of plastic-degrading genes provided strong indication of microbial populations that can putatively drive bioplastic biodegradation in the Baltic Sea. Populations with active plastic-degrading genes included common members of the marine plastisphere such as *Hyphomonas* (Alphaproteobacteria), *Sessilibacter*, and *Simiduia* (both Gammaproteobacteria) [24, 25, 27, 31], but also typically terrestrial taxa such as *Microbacterium* (Actinobacteria), *Acidovorax,* and *Hydrogenophaga* (both Gammaproteobacteria) that are generally common in coastal waters and estuaries [82–84]. Our results are thus likely relevant to other coastal and estuarine systems, but differences are expected since biogeographical and environmental factors are known to influence the composition of the plastisphere [22–26].

Metabolic reconstruction revealed that the active bioplastisphere comprised mainly aerobic and facultative anaerobic heterotrophs that encode the potential to degrade complex carbohydrates and polymers. The bioplastisphere populations were also enriched in anaerobic and nitrogen cycle traits compared to the non-biodegradable plastics. Our results indicate that nitrogen fixation might be an important strategy to counterbalance nitrogen deficiency when growing on the carbon-rich bioplastic materials [17, 28, 85]. Together with the increased capacity for anaerobic respiration via denitrification, these results also suggest that biofilm development on biodegradable plastics promotes low-oxygen microhabitats that favour facultative anaerobes [17, 28]. In addition, our results indicate that most bioplastisphere denitrifier populations have truncated pathways, as has been observed for other marine as well as terrestrial ecosystems [86, 87], and included populations with putative truncated pathways leading to nitrous oxide release. In all, our study suggests that the bioplastisphere populations encoding the potential to degrade bioplastics are microbial generalists adapted to a range of oxygen, carbon, and nutrient availabilities, with diverse couplings to the overall marine carbon and nitrogen cycles.

Our study suggests that bioplastic biodegradability might be on itself a stronger driver of microbial community composition than specific physicochemical properties of the plastic materials, with the carbon derived from the breakdown of different bioplastics maintaining a specialised bioplastisphere. Our study emphasizes the need to develop more robust industrial regulations that consider more broadly the issue of mismanaged bioplastic waste that ends up in the marine environment, where biodegradation happens much slowly. Although the search for marine biodegradable plastics and further characterisation of the bioplastisphere is an important way forward to mitigate plastic pollution, focus should be put in ensuring proper disposal of plastic waste and reducing plastic production at the source, which would also alleviate energy demands and greenhouse gas emissions.

Author contributions

ISP: Formal analysis, Software, Visualization, Writing – original draft, Writing – review & editing. **EE-R:** Conceptualization, Funding acquisition, Investigation, Writing – review & editing. **PN:** Investigation, Writing – review & editing. **DNT:** Conceptualization, Funding acquisition, Investigation, Writing – review & editing. **HK:** Conceptualization, Funding acquisition, Investigation, Project administration, Writing – review & editing.

Conflicts of interest

The authors declare no conflict of interest.

Acknowledgements

We thank Anna Kangas, Anni Jylhä-Vuorio, and Elisa Sillförs for help with the experimental work; Murat Eren, Iva Veseli, Florian Trigodet, Tom Delmont, and Laura Cappelatti for interesting discussions and ideas; and Minna Maunula and the students of the Microbiologist's Toolkit course (Autumn 2025, University of Helsinki) for insightful feedback on an earlier version of the manuscript. We acknowledge the DNA Sequencing and Genomics Laboratory (Institute of Biotechnology, University of Helsinki) for sequencing and the CSC–IT Centre for Finland for the computing infrastructure.

Study funding

This study was supported by the Research Council of Finland (grant number 332174).

Data availability

The metagenomic and metatranscriptomic data for this study have been deposited in the European Nucleotide Archive (ENA) at EMBL-EBI under the accession number PRJEB98035 (ebi.ac.uk/ena/browser/view/PRJEB98035). The data is currently under embargo and will be made public upon publication of the study.

Supplementary material

Pessi_et_al_2025_Suppl_Figs.docx: Supplementary figures S1–S11.

Pessi_et_al_2025_Suppl_Tables.xlsx: Supplementary tables S1–S2.

References

1. Jambeck JR et al. Plastic waste inputs from land into the ocean. *Science* 2015;**347**:768–771. https://doi.org/10.1126/science.1260352
2. Lebreton LCM et al. River plastic emissions to the world's oceans. *Nat Commun* 2017;**8**:15611. https://doi.org/10.1038/ncomms15611
3. Meijer LJJ et al. More than 1000 rivers account for 80% of global riverine plastic emissions into the ocean. *Sci Adv* 2021;**7**:eaaz5803. https://doi.org/10.1126/sciadv.aaz5803
4. Andrady AL. Persistence of plastic litter in the oceans. In: Bergmann M, Gutow L, Klages M (eds), Marine anthropogenic litter. Cham: Springer International Publishing, 2015, 57–72.
5. Napper IE, Thompson RC. Plastic debris in the marine environment: History and future challenges. *Global Chall* 2020;**4**:1900081. https://doi.org/10.1002/gch2.201900081
6. Tekman MB et al. Impacts of plastic pollution in the oceans on marine species, biodiversity and ecosystems. WWF, 2022. https://doi.org/10.5281/zenodo.5898684
7. Lebreton L, Andrady A. Future scenarios of global plastic waste generation and disposal. *Palgrave Commun* 2019;**5**:6. https://doi.org/10.1057/s41599-018-0212-7
8. Int-Veen I et al. Positively buoyant but sinking: Polymer identification and composition of marine litter at the seafloor of the North Sea and Baltic Sea. *Mar Pollut Bull* 2021;**172**:112876. https://doi.org/10.1016/j.marpolbul.2021.112876
9. Jylhä-Vuorio A et al. Incorporation of plastic debris into the nests of great cormorants (*Phalacrocorax carbo sinensis*) in the Gulf of Finland. *Mar Pollut Bull* 2024;**208**:116934. https://doi.org/10.1016/j.marpolbul.2024.116934
10. European Commission. Biodegradability of plastics in the open environment. European Commission, 2020. https://data.europa.eu/doi/10.2777/690248
11. European Commission. Requirements for packaging recoverable through composting and biodegradation: Test scheme and evaluation criteria for the final acceptance of packaging. European Commission, 2000. http://data.europa.eu/eli/dec/2001/524
12. Venâncio C, Lopes I, Oliveira M. Bioplastics: Known effects and potential consequences to marine and estuarine ecosystem services. *Chemosphere* 2022;**309**:136810. https://doi.org/10.1016/j.chemosphere.2022.136810
13. Lott C et al. Half-life of biodegradable plastics in the marine environment depends on material, habitat, and climate zone. *Front Mar Sci* 2021;**8**:662074. https://doi.org/10.3389/fmars.2021.662074
14. Choe S et al. Bridging three gaps in biodegradable plastics: Misconceptions and truths about biodegradation. *Front Chem* 2021;**9**:671750. https://doi.org/10.3389/fchem.2021.671750
15. Carpenter EJ et al. Polystyrene spherules in coastal waters. *Science* 1972;**178**:749–750. https://doi.org/10.1126/science.178.4062.749

16. Zettler ER, Mincer TJ, Amaral-Zettler LA. Life in the “plastisphere”: Microbial communities on plastic marine debris. *Environ Sci Technol* 2013;**47**:7137–7146. https://doi.org/10.1021/es401288x

17. Amaral-Zettler LA, Zettler ER, Mincer TJ. Ecology of the plastisphere. *Nat Rev Microbiol* 2020;**18**:139–151. https://doi.org/10.1038/s41579-019-0308-0

18. Lobelle D, Cunliffe M. Early microbial biofilm formation on marine plastic debris. *Mar Pollut Bull* 2011;**62**:197–200. https://doi.org/10.1016/j.marpolbul.2010.10.013

19. Dussud C et al. Colonization of non-biodegradable and biodegradable plastics by marine microorganisms. *Front Microbiol* 2018;**9**:1571. https://doi.org/10.3389/fmicb.2018.01571

20. Wright RJ et al. Marine plastic debris: A new surface for microbial colonization. *Environ Sci Technol* 2020;**54**:11657–11672. https://doi.org/10.1021/acs.est.0c02305

21. Cheng J et al. Relative influence of plastic debris size and shape, chemical composition and phytoplankton-bacteria interactions in driving seawater plastisphere abundance, diversity and activity. *Front Microbiol* 2021;**11**:610231. https://doi.org/10.3389/fmicb.2020.610231

22. Oberbeckmann S et al. Spatial and seasonal variation in diversity and structure of microbial biofilms on marine plastics in Northern European waters. *FEMS Microbiol Ecol* 2014;**90**:478–492. https://doi.org/10.1111/1574-6941.12409

23. Oberbeckmann S, Osborn AM, Duhaime MB. Microbes on a bottle: Substrate, season and geography influence community composition of microbes colonizing marine plastic debris. *PLoS ONE* 2016;**11**:e0159289. https://doi.org/10.1371/journal.pone.0159289

24. Oberbeckmann S, Kreikemeyer B, Labrenz M. Environmental factors support the formation of specific bacterial assemblages on microplastics. *Front Microbiol* 2018;**8**:2709. https://doi.org/10.3389/fmicb.2017.02709

25. Oberbeckmann S, Labrenz M. Marine microbial assemblages on microplastics: Diversity, adaptation, and role in degradation. *Annu Rev Mar Sci* 2020;**12**:209–232. https://doi.org/10.1146/annurev-marine-010419-010633

26. Amaral-Zettler LA et al. The biogeography of the plastisphere: Implications for policy. *Frontiers Ecol Environ* 2015;**13**:541–546. https://doi.org/10.1890/150017

27. Rogers KL et al. Micro-by-micro interactions: How microorganisms influence the fate of marine microplastics. *Limnol Oceanogr Lett* 2020;**5**:18–36. https://doi.org/10.1002/lol2.10136

28. Fortin SG et al. Microplastic biofilms as potential hotspots for plastic biodegradation and nitrogen cycling: a metagenomic perspective. *FEMS Microbiol Ecol* 2025;**101**:fiaf035. https://doi.org/10.1093/femsec/fiaf035

29. Morohoshi T et al. Molecular characterization of the bacterial community in biofilms for degradation of poly(3-hydroxybutyrate-*co*-3-hydroxyhexanoate) films in seawater. *Microbes Environ* 2018;**33**:19–25. https://doi.org/10.1264/jsme2.ME17052

30. Pinnell LJ, Turner JW. Shotgun metagenomics reveals the benthic microbial community response to plastic and bioplastic in a coastal marine environment. *Front Microbiol* 2019;**10**:1252. https://doi.org/10.3389/fmicb.2019.01252

31. Eronen-Rasimus EL, Näkki PP, Kaartokallio HP. Degradation rates and bacterial community compositions vary among commonly used bioplastic materials in a brackish marine environment. *Environ Sci Technol* 2022;**56**:15760−15769. https://doi.org/10.1021/acs.est.2c06280

32. Dimassi SN et al. Insights into the degradation mechanism of PET and PP under marine conditions using FTIR. *J Hazard Mater* 2023;**447**:130796. https://doi.org/10.1016/j.jhazmat.2023.130796

33. ASTM. Standard test method for determining aerobic biodegradation of plastic materials in the marine environment by a defined microbial consortium or natural sea water inoculum. ASTM, 2017. https://store.astm.org/d6691-17.html

34. Goudriaan M et al. A stable isotope assay with 13^{C}-labeled polyethylene to investigate plastic mineralization mediated by *Rhodococcus ruber*. *Mar Pollut Bull* 2023;**186**:114369. https://doi.org/10.1016/j.marpolbul.2022.114369

35. De Vogel FA et al. Biodegradable plastics in Mediterranean coastal environments feature contrasting microbial succession. *Sci Total Environ* 2024;**928**:172288. https://doi.org/10.1016/j.scitotenv.2024.172288

36. Sun Y et al. Distinct microbial communities degrade cellulose diacetate bioplastics in the coastal ocean. *Appl Environ Microbiol* 2023;**89**:e01651-23. https://doi.org/10.1128/aem.01651-23

37. Omura T et al. Microbial decomposition of biodegradable plastics on the deep-sea floor. *Nat Commun* 2024;**15**:568. https://doi.org/10.1038/s41467-023-44368-8

38. Feijoo P et al. Marine degradation of plastics in Western Mediterranean Sea: Comparison between biodegradable and conventional polymers. *Polym Degrad Stab* 2025;**234**:111222. https://doi.org/10.1016/j.polymdegradstab.2025.111222

39. Deroiné M et al. Natural degradation and biodegradation of poly(3-hydroxybutyrate-co-3-hydroxyvalerate) in liquid and solid marine environments. *J Polym Environ* 2015;**23**:493–505. https://doi.org/10.1007/s10924-015-0736-5

40. Kirstein IV et al. Mature biofilm communities on synthetic polymers in seawater - Specific or general? *Mar Environ Res* 2018;**142**:147–154. https://doi.org/10.1016/j.marenvres.2018.09.028

41. Kirstein IV et al. The plastisphere – Uncovering tightly attached plastic "specific" microorganisms. *PLoS ONE* 2019;**14**:e0215859. https://doi.org/10.1371/journal.pone.0215859

42. Connors E et al. Changes in microbial community structure of bio-fouled polyolefins over a year-long seawater incubation in Hawai'i. *Environ Microbiol Rep* 2024;**16**:e13283. https://doi.org/10.1111/1758-2229.13283

43. Scott J et al. Systematic critical review of studies and methods assessing microbial degradation of plastics in the marine environment: Evidence base and

641 recommendations. *Sci Total Environ* 2025;**999**:180277.
642 https://doi.org/10.1016/j.scitotenv.2025.180277

643 44. Bryant JA et al. Diversity and activity of communities inhabiting plastic debris in
644 the North Pacific Gyre. *mSystems* 2016;**1**:e00024-16.
645 https://doi.org/10.1128/msystems.00024-16

646 45. Seeley ME et al. Microplastics affect sedimentary microbial communities and
647 nitrogen cycling. *Nat Commun* 2020;**11**:2372. https://doi.org/10.1038/s41467-020-
648 16235-3

649 46. Pang R et al. Genome-centric metagenomics insights into the plastisphere-driven
650 natural degradation characteristics and mechanism of biodegradable plastics in
651 aquatic environments. *Environ Sci Technol* 2024;**58**:18915–18927.
652 https://doi.org/10.1021/acs.est.4c04965

653 47. Zhou L et al. From waste to resource: Metagenomics uncovers the molecular
654 ecological resources for plastic degradation in estuaries of South China. *Water Res*
655 2023;**242**:120270. https://doi.org/10.1016/j.watres.2023.120270

656 48. Agilent. MicroLab. v5.8, 2024. https://www.agilent.com/en/product/molecular-
657 spectroscopy/ftir-spectroscopy/ftir-software/microlab-ftir-software

658 49. Viitamäki S et al. The activity and functions of soil microbial communities in the
659 Finnish sub-Arctic vary across vegetation types. *FEMS Microbiol Ecol*
660 2022;**98**:fiac079. https://doi.org/10.1093/femsec/fiac079

661 50. Martin M. Cutadapt removes adapter sequences from high-throughput sequencing
662 reads. *EMBnet J* 2011;**17**:10. https://doi.org/10.14806/ej.17.1.200

663 51. Andrews S. FastQC: A quality control tool for high throughput sequence data.
664 v0.12.1, 2019. http://www.bioinformatics.babraham.ac.uk/projects/fastqc

665 52. Ewels P et al. MultiQC: Summarize analysis results for multiple tools and samples
666 in a single report. *Bioinformatics* 2016;**32**:3047–3048.
667 https://doi.org/10.1093/bioinformatics/btw354

668 53. Menzel P, Ng KL, Krogh A. Fast and sensitive taxonomic classification for
669 metagenomics with Kaiju. *Nat Commun* 2016;**7**:11257.
670 https://doi.org/10.1038/ncomms11257

671 54. Woodcroft BJ et al. Comprehensive taxonomic identification of microbial species in
672 metagenomic data using SingleM and Sandpiper. *Nat Biotechnol* 2025;**in press**.
673 https://doi.org/10.1038/s41587-025-02738-1

674 55. Parks DH et al. GTDB: An ongoing census of bacterial and archaeal diversity
675 through a phylogenetically consistent, rank normalized and complete genome-based
676 taxonomy. *Nucleic Acids Res* 2022;**50**:D785–D794.
677 https://doi.org/10.1093/nar/gkab776

678 56. Eren AM et al. Community-led, integrated, reproducible multi-omics with anvi'o.
679 *Nat Microbiol* 2021;**6**:3–6. https://doi.org/10.1038/s41564-020-00834-3

680 57. Li D et al. MEGAHIT: An ultra-fast single-node solution for large and complex
681 metagenomics assembly via succinct de Bruijn graph. *Bioinformatics* 2015;**31**:1674–
682 1676. https://doi.org/10.1093/bioinformatics/btv033

683 58. Hyatt D et al. Prodigal: Prokaryotic gene recognition and translation initiation site
684 identification. *BMC Bioinform* 2010;**11**:119. https://doi.org/10.1186/1471-2105-11-
685 119

686 59. Lee MD. GToTree: A user-friendly workflow for phylogenomics. *Bioinformatics*
687 2019;**35**:4162–4164. https://doi.org/10.1093/bioinformatics/btz188

688 60. Eddy SR. Accelerated profile HMM searches. *PLoS Comput Biol* 2011;**7**:e1002195.
689 https://doi.org/10.1371/journal.pcbi.1002195

690 61. Buchfink B, Xie C, Huson DH. Fast and sensitive protein alignment using
691 DIAMOND. *Nat Methods* 2015;**12**:59–60. https://doi.org/10.1038/nmeth.3176

692 62. Langmead B, Salzberg SL. Fast gapped-read alignment with Bowtie 2. *Nat Methods*
693 2012;**9**:357–359. https://doi.org/10.1038/nmeth.1923

694 63. Li H et al. The Sequence Alignment/Map format and SAMtools. *Bioinformatics*
695 2009;**25**:2078–2079. https://doi.org/10.1093/bioinformatics/btp352

696 64. Kang DD et al. MetaBAT 2: An adaptive binning algorithm for robust and efficient
697 genome reconstruction from metagenome assemblies. *PeerJ* 2019;**7**:e7359.
698 https://doi.org/10.7717/peerj.7359

699 65. Jain C et al. High throughput ANI analysis of 90K prokaryotic genomes reveals
700 clear species boundaries. *Nat Commun* 2018;**9**:5114. https://doi.org/10.1038/s41467-
701 018-07641-9

702 66. Olm MR et al. dRep: A tool for fast and accurate genomic comparisons that enables
703 improved genome recovery from metagenomes through de-replication. *ISME J*
704 2017;**11**:2864–2868. https://doi.org/10.1038/ismej.2017.126

705 67. Chaumeil P-A et al. GTDB-Tk v2: Memory friendly classification with the genome
706 taxonomy database. *Bioinformatics* 2022;**38**:5315–5316.
707 https://doi.org/10.1093/bioinformatics/btac672

708 68. Aroney STN et al. CoverM: Read alignment statistics for metagenomics.
709 *Bioinformatics* 2025;**41**:btaf147. https://doi.org/10.1093/bioinformatics/btaf147

710 69. Aramaki T et al. KofamKOALA: KEGG ortholog assignment based on profile HMM
711 and adaptive score threshold. *Bioinformatics* 2020;**36**:2251–2252.
712 https://doi.org/10.1093/bioinformatics/btz859

713 70. Drula E et al. The carbohydrate-active enzyme database: Functions and literature.
714 *Nucleic Acids Res* 2022;**50**:D571–D577. https://doi.org/10.1093/nar/gkab1045

715 71. Gambarini V et al. PlasticDB: A database of microorganisms and proteins linked to
716 plastic biodegradation. *Database* 2022;**2022**:baac008.
717 https://doi.org/10.1093/database/baac008

72. Karaoz U, Brodie EL. microTrait: A toolset for a trait-based representation of microbial genomes. *Front Bioinform* 2022;**2**:918853. https://doi.org/10.3389/fbinf.2022.918853

73. R Core Team. R: A language and environment for statistical computing. v4.3.3, 2024. https://www.r-project.org

74. Lenth RV. emmeans: Estimated marginal means, aka least-squares means. v1.10.6, 2024. https://CRAN.R-project.org/package=emmeans

75. Hothorn T, Bretz F, Westfall P. multcomp: Simultaneous inference in general parametric models. v1.4.26, 2024. https://CRAN.R-project.org/package=multcomp

76. Oksanen J et al. vegan: Community ecology package. v2.7.1, 2025. https://cran.r-project.org/package=vegan

77. Mallick H et al. Multivariable association discovery in population-scale meta-omics studies. *PLoS Comput Biol* 2021;**17**:e1009442. https://doi.org/10.1371/journal.pcbi.1009442

78. Mayumi D et al. Identification and characterization of novel poly(dl-lactic acid) depolymerases from metagenome. *Appl Microbiol Biotechnol* 2008;**79**:743–750. https://doi.org/10.1007/s00253-008-1477-3

79. Tachibana Y et al. Can poly(butylene succinate) degrade in seawater? *Chemosphere* 2025;**374**:144203. https://doi.org/10.1016/j.chemosphere.2025.144203

80. Beiras R, López-Ibáñez S. A practical tool for the assessment of polymer biodegradability in marine environments guides the development of truly biodegradable plastics. *Polymers* 2023;**15**:974. https://doi.org/10.3390/polym15040974

81. Ridley RS et al. Potential routes of plastics biotransformation involving novel plastizymes revealed by global multi-omic analysis of plastic associated microbes. *Sci Rep* 2024;**14**:8798. https://doi.org/10.1038/s41598-024-59279-x

82. Zeghal E et al. Environmental factors control microbial colonization of plastics in the North Sea. *Mar Pollut Bull* 2024;**208**:116964. https://doi.org/10.1016/j.marpolbul.2024.116964

83. Wang Z et al. *Acidovorax* PSJ13, a novel, efficient polyacrylamide-degrading bacterium by cleaving the main carbon chain skeleton without the production of acrylamide. *Biodegradation* 2023;**34**:581–595. https://doi.org/10.1007/s10532-023-10036-3

84. Hansen J et al. Effect of polymer type on the colonization of plastic pellets by marine bacteria. *FEMS Microbiol Lett* 2021;**368**:fnab026. https://doi.org/10.1093/femsle/fnab026

85. Du Y et al. A review on marine plastisphere: Biodiversity, formation, and role in degradation. *Comput Struct Biotechnol J* 2022;**20**:975–988. https://doi.org/10.1016/j.csbj.2022.02.008

86. Rasigraf O et al. Microbial community composition and functional potential in Bothnian Sea sediments is linked to Fe and S dynamics and the quality of organic matter. *Limnol Oceanogr* 2020;**65**:S113–S133. https://doi.org/10.1002/lno.11371

87. Pessi IS et al. In-depth characterization of denitrifier communities across different soil ecosystems in the tundra. *Environ Microbiome* 2022;**17**:30. https://doi.org/10.1186/s40793-022-00424-2